JOURNAL OF MATERIALS SCIENCE 31 (1996) 1165–1173

Fibre interactions in two-dimensional composites by micro-Raman spectroscopy

H.D. WAGNER*
Department of Materials & Interfaces, Weizmann Institute of Science, Rehovot 76100, Israel
M.S. AMER, L.S. SCHADLER
Department of Materials Engineering, Drexel University, Philadelphia, PA 19104–9984, USA

In the study of fracture processes in composite materials, the interactions between broken and intact fibres are of critical importance. Indeed, the redistribution of stress from a failed fibre to its unfailed adjacent neighbours, and the stress concentration induced in these, determine the extent to which a break in one fibre will cause more breaks in neighbouring fibres. The overall failure pattern is a direct function of the stress concentration factors. In this paper we use laser micro-Raman spectroscopy to study the extent of stress transfer and redistribution caused by fibre fracture in two-dimensional Kevlar 149 based microcomposites. The strain along the fibres was mapped at different levels of load, and specimens with different inter-fibre distances were used to study the fibre content effect. The experimental stress concentration factors were compared with values predicted from various theoretical models. The stress concentration factors generally agreed with those literature models that include interfibre distance and matrix effects. The overall failure pattern was found not to be a direct function of the stress concentration factors in this system, as fracture propagates from fibre to fibre even at large interfibre distances, and is apparently accompanied by relatively low values of the stress concentration factors. The 'critical cluster size', beyond which final fracture of the composite occurs in a catastrophic manner, was found to be larger than five adjacent fibre breaks in the present system, for all interfibre distances studied.

1. Introduction

1.1. Theoretical aspects

The understanding of fibre–fibre interactions is a fundamental matter in the study of fracture processes in composite materials. Basic arguments and relevant references concerning this issue are included in previous work [1, 2]. Consider a thin matrix film reinforced by fibres disposed unidirectionally, in which a tensile stress field is applied parallel to the fibre axis. As a result of the strength variability of the single fibres (both from point to point within the fibre length, and from fibre to fibre), breaks appear randomly at fibre sites where the applied stress exceeds the local strength. When the fibre content is relatively large (thus, when the fibre to fibre distance is small), an intact fibre section adjacent to a neighbouring broken fibre section will experience an additional stress due to the load released by the broken fibre. In the case of a loose fibre bundle (no matrix present) the surviving fibres most probably share equally all the released stress, a situation which was analysed by Daniels [3] in a classical study. However, in a composite, the presence of the matrix, and the strength of the interfacial bond, bias the way the load released is shared by the intact fibres, and it is experimentally observed that the surviving fibres closer to a broken fibre absorb more of the released load. Indeed, one usually observes clusters of adjacent fibre breaks, the size of which is variable but usually limited to at most 5–10 adjacent breaks. Thus in composite materials the stress released by broken fibres is shared **locally** by adjacent fibres rather than **equally** by all fibres.

To conveniently express the overloading in an intact fibre resulting from the load released by a broken fibre, a stress concentration factor (SCF) is defined as the ratio between the local stress in the intact fibre (σ_{local}) and the applied stress in the fibre far away from a break ($\sigma_{applied}$). Thus,

$$K = \frac{\sigma_{local}}{\sigma_{applied}} \quad (1)$$

Since σ_{local} is composed of the applied stress $\sigma_{applied}$ plus the extra stress σ_{extra} released by the fibre break, the SCF can be expressed as

$$K = 1 + \frac{\sigma_{extra}}{\sigma_{applied}} \quad (2)$$

* Visiting Stein Fellow at Drexel University, July-September 1994.

0022–2461

A pioneering study of the overloading in an intact fibre was performed by Hedgepeth [4] followed by that of Hedgepeth and Van Dyke [5], who used a shear–lag approach to determine the average SCF in a fibre, due to q adjacent breaks in a two dimensional composite material. Their expression for the (static) SCF was

$$K_q^{(s)} = \prod_{j=1}^{q} \frac{2j+2}{2j+1} \tag{3}$$

As seen, Hedgepeth's SCF is independent of the inter-fibre distance (or the fibre content), and of the physical properties of the fibre and the matrix. The length scale for the overload, however, does depend on these quantities, and that affects fibre fracture statistics. In the special case of simultaneous failure of q adjacent fibres, a dynamic SCF was defined as $K_q^{(d)} = \eta_q K_q^{(s)}$, where $1.15 \leq \eta_q < 1.27$. Equation 3 is still widely used by most researchers in the composite materials field. Fichter [6] extended this analysis to the case of two collinear, separated clusters of fibre breaks each having a variable size. To simplify probabilistic calculations of fracture, Harlow and Phoenix [7, 8] proposed a local load sharing rule such that the load released by the broken fibre is only transferred to the two nearest neighbouring fibres. This extreme situation is reflected by the following rule for the SCF in a surviving fibre:

$$K_q = 1 + \frac{q}{2} \tag{4}$$

where again q is the number of adjacent failed fibres. As in the previous case (Equation 3) the SCF is given by a mathematical rule that does not include the experimentally observed effects of fibre content and material properties of the constituents. Pitt and Phoenix [9, 10] later proposed "tapered" load-sharing rules whereby not all of the redistributed load goes onto the nearest neighbours of the broken fibre. Smith *et al.* [11] extended this to the case of a hexagonal bundle. However, as in previous works, materials and geometrical constants do not appear in the proposed rules.

An analytical model proposed by Fukuda and Kawata [12–14] included for the first time the effect of material parameters on the SCF, through the ratio E_f/E_m, where E is Young's modulus, and the subscripts f and m designate the fibre and the matrix, respectively. The effect of the fibre content V_f also appears in the analysis. In contrast with Hedgepeth's analysis, the matrix is assumed to bear both shear and tensile stresses (Hedgepeth assumed that the matrix is loaded in shear only). The numerical results obtained in the study of Fukuda and Kawata were presented in graphical form and showed that the SCF increases with decreasing interfibre distance, with increasing value of the ratio E_f/E_m, and with the number of adjacent broken fibres. As the number of broken fibres, q, increased, Fukuda and Kawata found their values of K_q to be progressively smaller than those of Hedgepeth and of Harlow and Phoenix. A more complex treatment has also been proposed by Rossettos and Shishesaz [15] involving accurate analysis of the stresses near fibre breaks.

Using a different approach, Bader *et al.* [16] assumed the SCF to take a "mixed" form

$$K_q = 1 + \frac{q^{1/2}}{F} \tag{5}$$

where F is an experimentally determined function of the inter-fibre distance, and is termed the load sharing factor. Thus, this is an approach which attempts to include, in a semi-empirical way, the effects of material and geometrical characteristics of the composite. Using the experimental data generated by Bader *et al.* [16–19], Wolstenholme and Smith [20] combined an analytical approach and experimental results to calculate the SCF, using Equation 5. A maximum likelihood method was used to determine the parameter F, based on the experimental results, and an optimal value of the SCF was calculated for different inter-fibre distances.

More recently, Eitan and Wagner [1, 2] developed a model for the SCF based on shear-lag concepts, for different cases of two-dimensional (planar) composites in which the fibres are aligned parallel to each other. The resulting SCF was an explicit function of the interfibre distance, the matrix and fibre properties, the number and position of broken fibres, the position along the fibre away from the break site, as well as the stress transfer length. The validity of the model was assessed by comparison with SiC/epoxy data inferred from the experiments of Bader *et al.* [16–19]. Possible sources of error in the model were briefly discussed. Overall, the local effect of fibre breaks on nearest neighbours was found to be milder than previously assumed. A recent three-dimensional finite element analysis by Nedele and Wisnom [21] for a single broken fibre surrounded by six equally spaced fibres (using a high volume fraction of 0.60) also resulted in relatively low values for the SCF.

1.2. Survey of recent experimental work

Until recently, no direct experimental confirmation existed addressing the validity and accuracy of the predicted values of the stress concentration factors. This situation has changed lately, following the emergence of two new classes of experimental tools: (i) highly accurate strain profile measurements by microscope Raman spectroscopy [22–24] and (ii) two-dimensional model composites, or microcomposites, in which very thin single fibres are accurately positioned and all geometrical, structural and manufacturing parameters can be fully controlled [25–28]. The first (and so far only) quantitative study of stress concentration factors in two-dimensional microcomposites by means of micro-Raman spectroscopy, was performed by Atallah and Galiotis [29] using Kevlar 49/epoxy microcomposites. These authors mapped the strain along individual fibres at different levels of load, for a constant average interfibre spacing of $\sim$140–150 μm (or 12 fibre diameters) fibre content of 0.6%. They found a value of $K \approx 1.8$ in the intact fibres as a result of an

adjacent fibre fracture. This is larger than what one would expect for such large interfibre distance and relatively mild levels of fibre–matrix adhesion, but may be the result of the thin specimens used.

1.3. Objectives of the present study

In this work, micro-Raman spectroscopy was employed to map the strain along individual, accurately positioned, Kevlar 149 fibres in a polymeric matrix. The main objective of the study was to detect possible load redistribution and sharing effects from a broken fibre onto its (still intact) near neighbours, and thereby to estimate the SCF in these. The effect of variable interfibre distance upon the SCF was also examined. Note that the microcomposites used here belong to a new family of such model composites, as they are prepared by means of uv-polymerization, a procedure that enables specimen making in only a few minutes (once the fibre array is ready), as compared to several hours in earlier work with epoxy resins.

2. Experimental details

2.1. Materials

The fibre material used in this study was Kevlar 149 aramid (Du Pont de Nemours Inc.), extracted from a spool containing 768 fibres per yarn. This fibre has a strain to failure of about 1.5%, a Young's modulus of 150–160 GPa, and a tensile strength of about 2.4 GPa. We chose to use this fibre rather than Kevlar 29 or Kevlar 49 because its lower strain to failure would enhance the extent of fibre fragmentation (in other words, the difference between the strain to failure of the fibre and that of the matrix would be even larger).

The matrix was a uv-curable polymer, the formulation of which consists of a commercially available urethane diacrylate oligomer, EBECRYL 4858 (Radcure Products, UBC Chemicals), and a benzyl ketal photoinitiator, IRGACURE 651 (Radcure Products, UBC Chemicals). This specific system was chosen because its stiffness (1.7 GPa) and tensile strength (49 MPa) are very similar to the epoxy system we used in our earlier studies, namely, DER 331 epoxy (DGEBA from Dow Chemical) and DEH 26 hardener (TEPA, also from Dow Chemical). An added advantage (regarding the fragmentation phenomenon) of this uv-curable system is its large failure strain of close to 20%, thus much larger than the fibre failure strain, which ensures that fragmentation indeed takes place.

2.2. Microcomposite preparation

As mentioned earlier, the microcomposites used in this work were prepared by means of uv-polymerization, a procedure that enables specimen preparation in only a few minutes (once the fibre array is ready), as compared to several hours (up to a day in some cases) in our earlier work with epoxy resins. Two-dimensional microcomposites containing five Kevlar 149 fibres were prepared. The fibre array was prepared using a home-made jig and following the procedure described by Wagner *et al.* [25, 26, 30, 31]. Approximately 50 g of the oligomer was held at 60 °C and combined with 2% bw of the photoinitiator. The mixture was thoroughly mixed at 60 °C for 30 min, and then cooled to room temperature. It was then spread onto the fibre array (supported by a rectangular pvc plate) using a blade, down to a thickness of approximately 100 μm. The plate was then placed on the conveyor of a mini conveyor curing unit (UV Process Supply, Inc.) and exposed five times successively to a 300 watt $inch^{-1}$ uv lamp, at a speed of 270 cm min^{-1}. The resulting polymerized specimens were defect free and of high quality. Following polymerization, the specimens were cut to size using a home made cutter [25, 30], and prepared for fragmentation testing as described elsewhere [25]. These microcomposite films were affixed to a dogbone-shaped epoxy substrate that fitted the clamping unit available at Drexel University, for further combined tensile and micro-Raman testing.

Specimens with five embedded fibres were prepared, using varying interfibre distances, as shown in Fig. 1. The fibre diameter varied somewhat from fibre to fibre, with an average value of 11.9 ± 0.6 μm. The average centre-to-centre interfibre distances (in units of average fibre diameter, D) were $2D \pm 0.33D$, $6D \pm 0.69D$, and 12D (no detectable error on the interfibre distance in the last case), respectively.

2.3. Fibre strain mapping by micro-Raman spectroscopy

Raman measurements were performed using a Jobin-Yvon micro-Raman spectrometer (model S3000, modified with a notch filter and spectrograph). The 514.5 nm line of an argon–ion laser was used to obtain the Raman spectra. The laser beam was focused to a 2 μm spot on the fibres using a modified Olympus microscope. Raman spectra were recorded using a charge coupled device (CCD). The peak positions were determined by fitting a Lorentzian function to the spectra. All Raman measurements were performed following the strain-sensitive Raman active peak near 1610 cm^{-1}, which reflects the distortion of the phenylene functional group. The strain dependence of the Raman peak position for aramid fibres was observed and reported previously [23, 29] and the peak position was found to shift linearly to lower values under tensile strain. The slope of this linear relationship, referred to as the Raman frequency gauge factor (RFGF), is unique for the same fibre and the same vibrational model. As seen in Fig. 2, where the 1610 cm^{-1} peak position is plotted against tensile strain, a straight line of slope RFGF $= -6.93$ $cm^{-1}\%^{-1}$ was found for Kevlar 149, using three single fibres. This is somewhat different from previously reported [23, 29] values (for Kevlar 49 fibres, however) of -4.1 to -4.4 $cm^{-1}\%^{-1}$.

Following preparation of the microcomposites, the Raman peak position was determined using steps of 100 μm along the length of the fibres. All five fibres in the three types of microcomposites were scanned, along a length of 4000 μm, at several load levels. Thus,

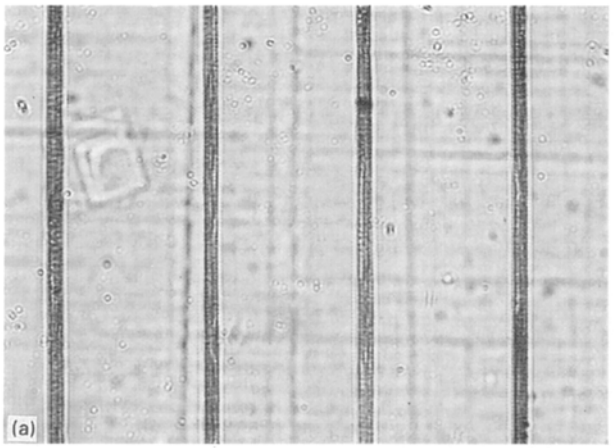

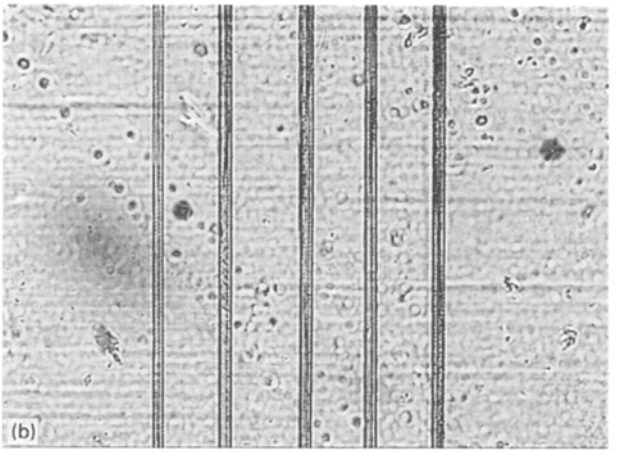

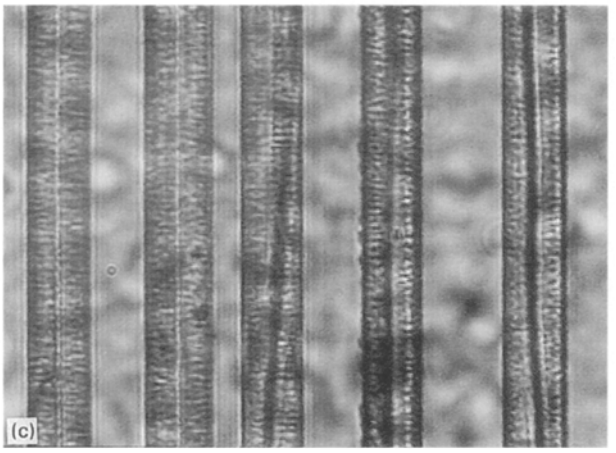

Figure 1 Optical microscope view of the three types of specimens studied in this work. The average diameter of the kevlar 149 fibres is 11.9 μm. The average centre-to-centre interfibre distances are (a) 143 μm; (b) 71 μm; and (c) 24 μm.

at each load level, 41 data points per fibre were collected, yielding a total of $41 \times 5 = 205$ data points for a given microcomposite at a given load level. Referring to Table I, which describes the work program in detail, a total of about 2000 micro-Raman data points were collected in this study. The axial strain in the fibre was calculated from the relationship

$$\varepsilon(x) = \frac{\nu(\varepsilon; x) - \nu(0; x)}{RFGF}$$

where $\varepsilon(x)$ is the fibre strain at point x, $\nu(\varepsilon; x)$ is the Raman frequency at the same point under strain ε, and $\nu(0; x)$ is the Raman frequency under no strain.

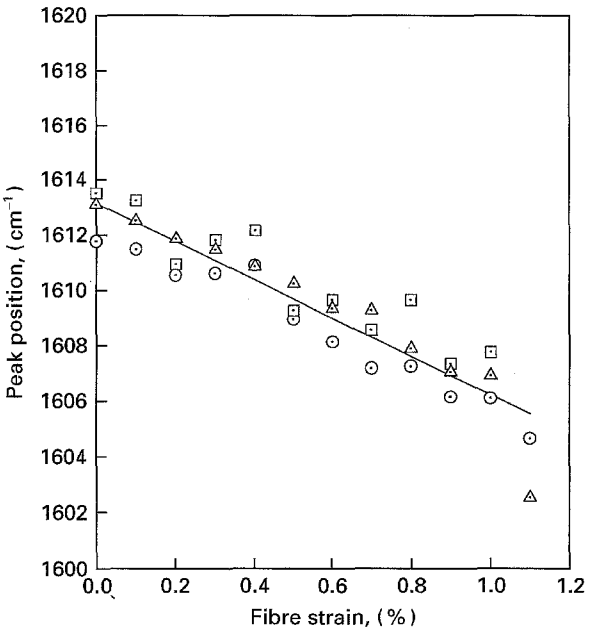

Figure 2 Rate of change of the 1610 cm^{-1} Raman peak position of kevlar 149, with respect to tensile strain, using three single fibres designated ⊙, ⊡ and △. A linear fit of slope RFGF = $-6.93\ cm^{-1}\ \%^{-1}$ is obtained.

TABLE I Summary of work program and fibre designation

Interfibre distance (centre-to-centre)	Strain level (%)	Fibre designation	Comments
12D	1.4	x1, x2, x3, x4, x5	—
12D	1.5	y1, y2, y3, y4, y5	—
12D	1.6	z1, z2, z3, z4, z5	scanning length of 3000 μm only
6D	1.3	a1, a2, a3, a4, a5	defect induced by laser burn in fibre a3
6D	1.4	b1, b2, b3, b4, b5	—
2D	1.3	11, 12, 13, 14, 15	—
2D	1.4	m1, m2, m3, m4, m5	—
2D	1.5	n1, n2, n3, n4, n5	—

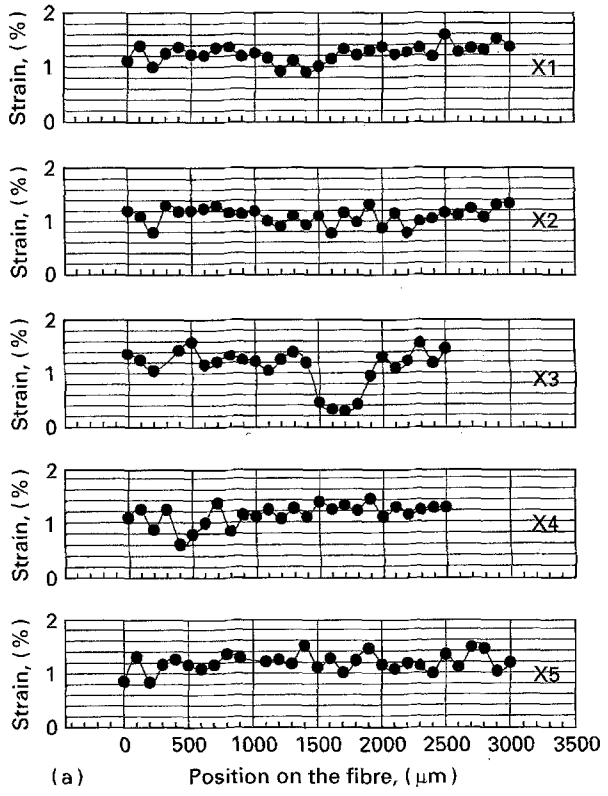

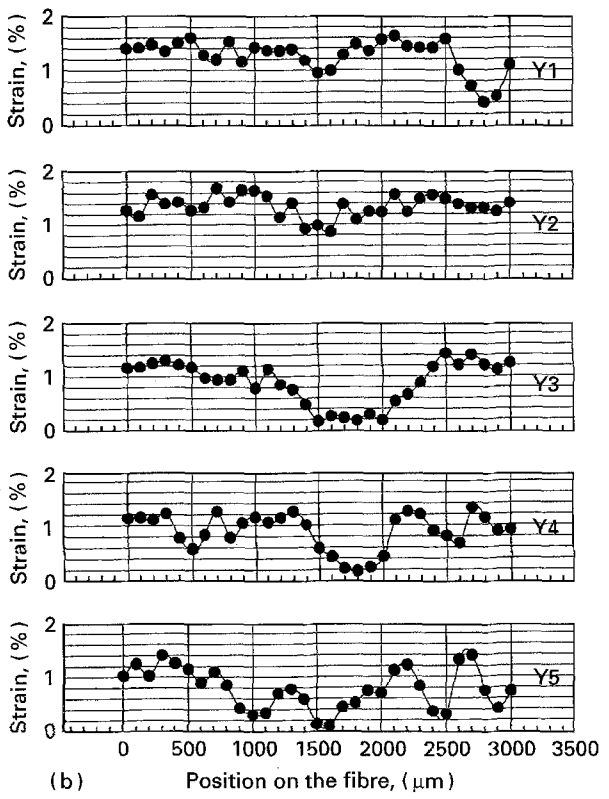

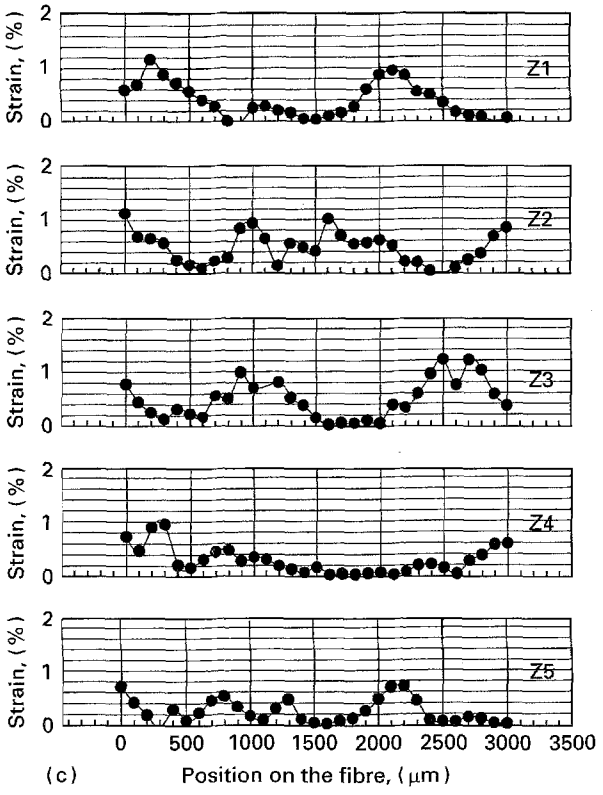

Figure 3 Strain mapping of the five kevlar 149 fibres in the microcomposites in which the average centre-to-centre interfibre distance is 12 fibre diameters. The applied strain is (a) 1.4%, (b) 1.5%, (c) 1.6%.

3. Results and discussion

3.1. General observations

Table I is a convenient summary of the work performed here. The microcomposites were progressively loaded under tensile stress parallel to the fibre direction. The general approach is similar to that used by Atallah and Galiotis [29] as 'observation windows' of up to 4000 μm length were used, the height of which included all five fibres in the composites.

The first fibre break could not easily be detected optically, both because the urethane–acrylate matrix material is not birefringent (unlike epoxy), and because it is inherently difficult to detect the nucleation of a break in kevlar. This created a practical difficulty as exhaustive straining and Raman mapping had to be performed at relatively low strain levels, until a break could be detected by Raman mapping. The strain at which first failure events occur in kevlar 149 was smaller than in kevlar 49 (1.4–1.5%, against about 1.8% in kevlar 49), as expected. All strain mapping results for the five fibres, in each specimen, are presented in Figs 3–5. Fig 5a is a good example of five yet unbroken fibres, at a centre-to-centre distance of 2D and under a 1.3% strain, from which it is seen that the strain variability along each fibre is no more than 0.2–0.3%. We also found that, sometimes, not all intact fibres in a specimen were loaded to exactly the same strain level, a possible indication of either fibre-to-fibre diameter variability, or of intrinsic single fibre property variability.

A quantitative study of the stress concentration factors, K_q, and of the "radius of influence" of an isolated fibre break upon its neighbouring fibres, must evolve from results at relatively small to moderate strain levels. There, only few, sporadic and distant breaks have appeared in each fibre so that, on average, mostly intact regions of fibres are adjacent to a broken fibre site, and the effects of overload, and interfibre distance, can be assessed.

On the other hand, at moderate to high strain levels, it becomes very difficult to observe localized strain

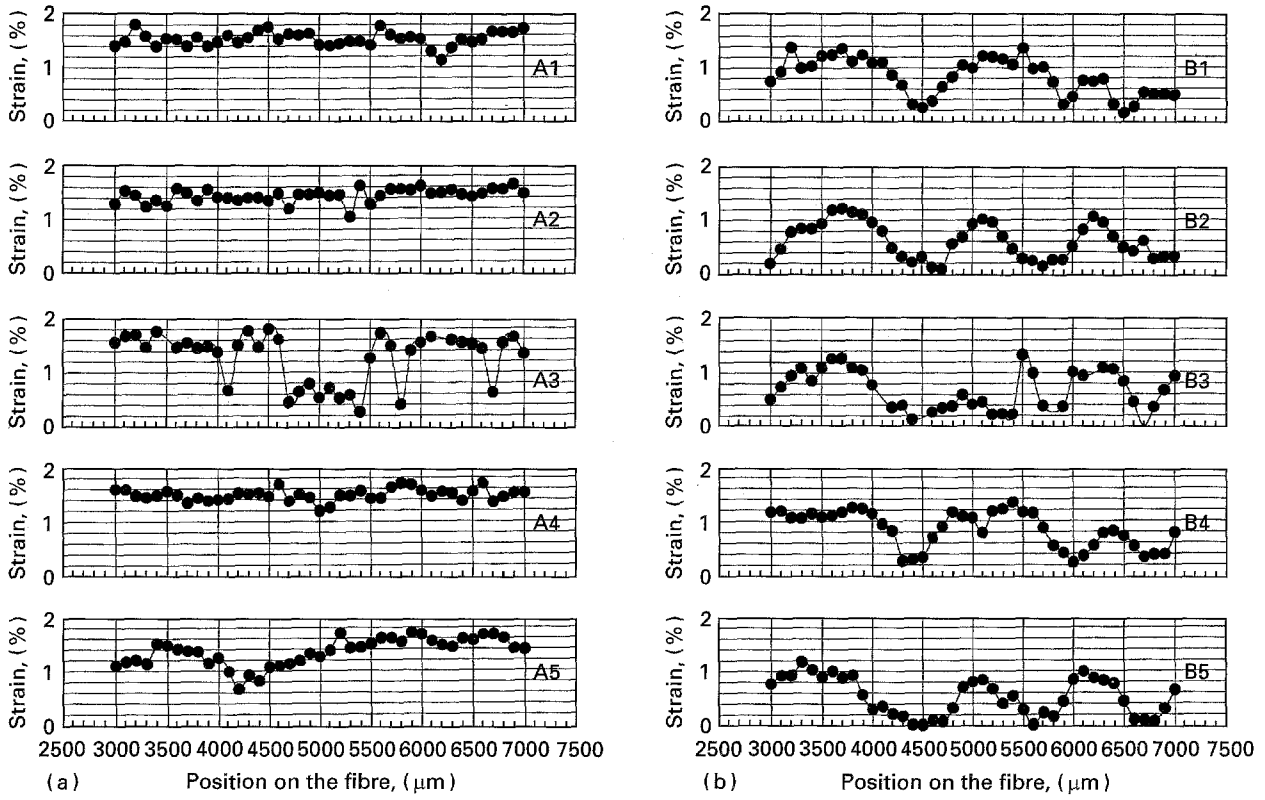

Figure 4 Strain mapping of the five kevlar 149 fibres in the microcomposites in which the average centre-to-centre interfibre distance is 6 fibre diameters. The applied strain is (a) 1.3%, (b) 1.4%.

increases in neighbouring fibres, close to a broken fibre, because the short-lived effect of such an overload has already led, in general, to the rupture of the neighbouring fibre or fibres. In the case of kevlar 149, as will be seen, this point is particularly critical. However, it is still possible, at such strain levels, to obtain useful information regarding the extent (or the lack) of fibre–fibre interaction as a function of inter-fibre distance, which is reflected by the size of a critical cluster of fibre breaks (by critical cluster size, we mean the number of adjacent broken fibres beyond which fast, catastrophic fracture of the composite section arises).

Note also that the type of load sharing rule in effect in a given composite material can in principle be determined, as a function of interfibre distance, by means of the information collected at both low and high load levels. This will be discussed further at a later stage.

3.2. Stress concentration factors K_q

Consider first the results under relatively small strain. As seen from Fig. 3a, at large interfibre distance (12D) and under 1.4% strain, some damage already exists in the specimen studied. A well developed fibre break is present in the central fibre (denoted X3), at the 1700 μm position, and some fluctuations are present along X3 as well as along all other four fibres. The length of the break zone, where the fibre supports no strain, is about 200–300 μm, and so is the length of the strain transfer zone, on each side of the break. Both these lengths increase with strain, as seen from Fig. 3(b, c). The length of the transfer zone around a break in a highly strained specimen can reach 500 μm and more. These observations are similar to those of Atallah and Galiotis [29] for kevlar 49. Of particular interest is what happens in the neighbouring fibres, adjacent to the major break in X3: nothing more than vague fluctuations in strain seem to result in fibres X2 and X4 from the break in X3, under 1.4% strain (Fig. 3a). This would imply that, as expected, for such a large inter-fibre distance, there is no stress concentration ($K_q \approx 1$). Another significant break develops under a strain of 1.5% in fibre Y1, at the 2800 μm position, and not much seems to happen in its neighbouring fibre Y2, at the same position: the small strain increase (which is in the error band) at 3000 μm, relative to the strain at 2800 or 2900 μm, would result in a strain concentration factor of at most 1.4/1.3 = 1.077. These observations are consistent with what theoretical models would predict at such large inferfibre distances [2, 12–14] (except for those models which do not include the interfibre distance as a variable [4, 5] and predict $K_1 = 1.33$), namely, a stress (or strain) concentration factor of close to 1, but they do contrast with the results of Atallah and Galiotis [29] who do observe very large values of K (from 1.4 to 1.8) in thin kevlar 49 based microcomposites with a similar interfibre distance of 12D.

When the centre-to-centre interfibre distance decreases to six fibre diameters, Fig. 4, no major difference arises regarding the strain concentration factors. Here, however, we induced an artificial fibre break in fibre A3 (at the 5000 μm position, Fig. 4a) by letting the laser spot burn the fibre, so as to avoid having to heavily scan the specimen fibres until a break was found. Note that the break has a different shape or profile, with a longer fracture zone and a rather sharp

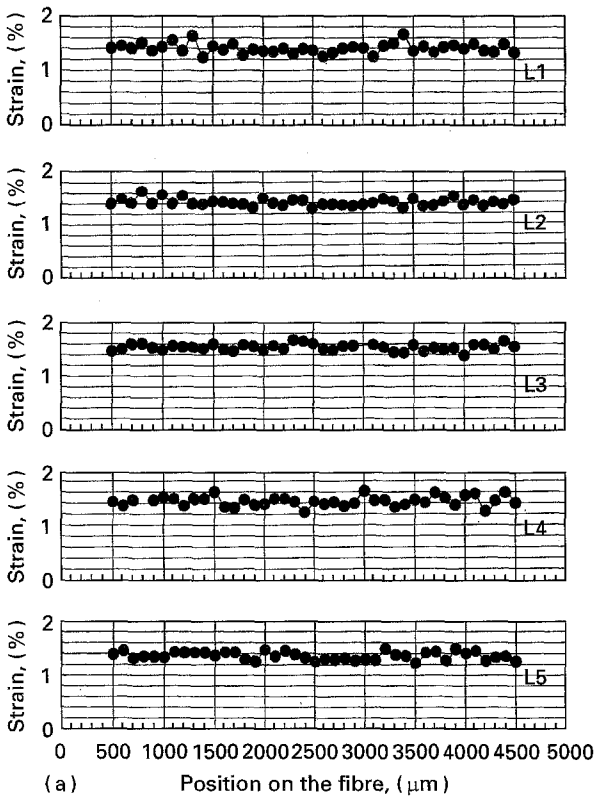

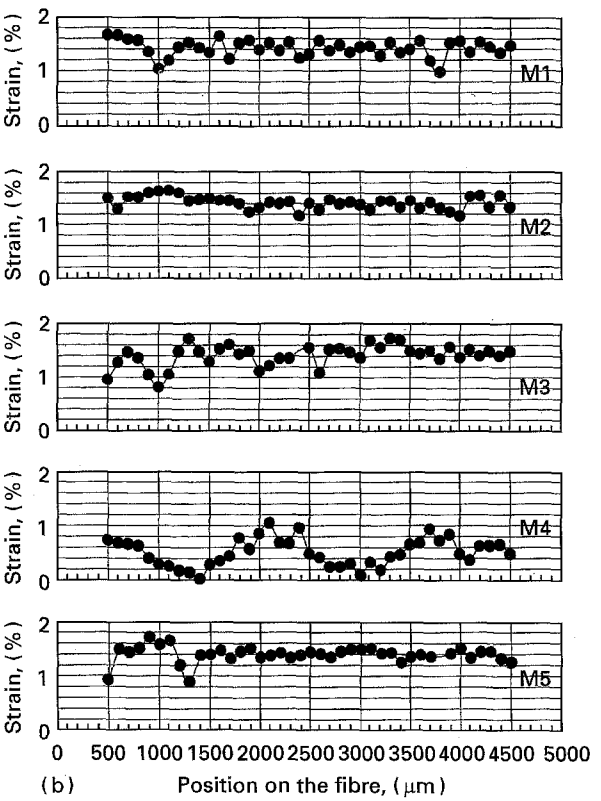

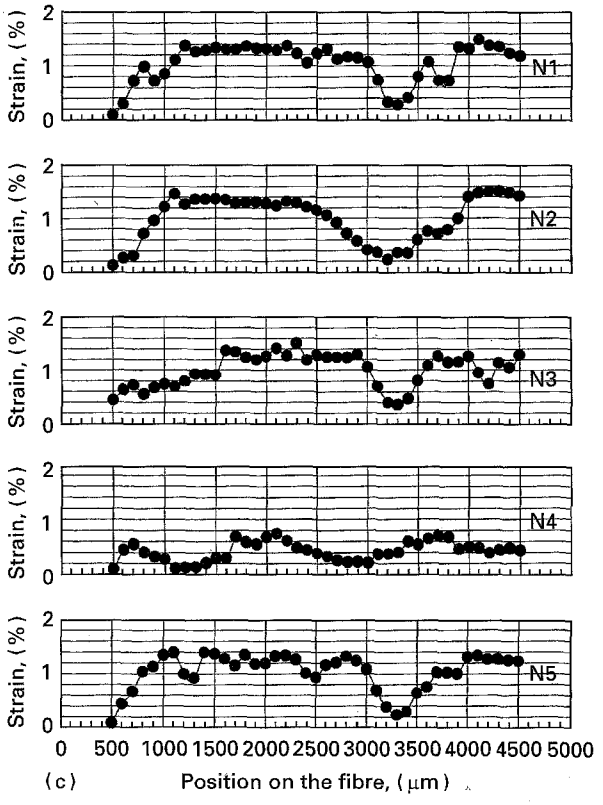

Figure 5 Strain mapping of the five kevlar 149 fibres in the microcomposites in which the average centre-to-centre interfibre distance is 2 fibre diameters. The applied strain is (a) 1.3%, (b) 1.4%, (c) 1.5%.

strain buildup zone, the latter being due to the comparatively sharp fracture edges resulting from burning, which contrasts with the well known fibrillar fracture of kevlar in stress-induced fibre breaks. However, looking at adjacent fibres A2 and A4, no strain concentration is observed at this (1.3%) strain level.

When the centre-to-centre distance is even smaller, down to two fibre diameters, no break at all is observed at 1.3% strain (Fig. 5a), but an interesting (and perhaps revealing) observation may be made at 1.4% strain (Fig. 5b): both fibres M1 and M3 break at exactly the same position (1000 μm), but the effect in the 'sandwiched' fibre M2 of this double break is barely a jump from 1.4% to 1.6%, which results in a strain concentration factor of 1.14. Such a fracture cluster geometry was considered by Fichter [6] and by Wagner and Eitan [2] (refer to their Table 2), whose calculated stress concentration factors are 1.714 and 1.161, respectively. The present experimental value does not compare well with Fichter's result, but compares favourably with that of Wagner and Eitan. The failure at the 1000 μm position, however, is not complete and thus the broken fibres are still carrying some load, which somewhat reduces the observed value of the strain concentration factor.

Another conclusion from the observations at relatively low strain is that the type of load redistribution rule that seems to be in effect in the kevlar based composite system examined here is probably close to an equal load sharing rule (ELS), by which the load released from a broken fibre is redistributed more or less equally (rather than locally) onto its nearest neighbours. This conclusion will be reinforced by the fracture mode observed at higher strain levels, as well as by earlier experimental observations [25] with kevlar 149/epoxy microcomposites. Note also that, based on our observations, it seems very difficult to conclude anything precise concerning the extent of the "zone (or radius) of influence" that arises from a fibre break in the present composite system.

3.3. Extent of fibre–fibre interactions and critical cluster size

Despite the fact that, as discussed above, the stress concentration factors are relatively small even when the fibres are very close to each other and the local fibre content is high, it is clearly observed from Figs 3–5 that at higher strains, there is excellent correlation between breaks in neighbouring fibres. In other words, fibre breaks in one fibre induce breaks in adjacent fibres at progressively higher strains, even though the apparent stress concentration factors are relatively small. Examples of such behaviour are (i) the cluster at 1600–1700 μm in the 12D interfibre distance composites, which appears at 1.5% and 1.6% strain; (ii) the two clusters at 4500 μm and 6500–6700 μm in the 6D interfibre distance composites, which appear at 1.4% strain; (iii) the cluster at 3300 μm in the 2D interfibre distance composites, which appears at 1.5% strain.

Thus, and as also previously observed (under polarized light) [25] in kevlar 149/epoxy microcomposites containing eight parallel fibres (with an interfibre distance of about 4–6D), fragmentation clusters appear across the entire section of the microcomposite, repeating themselves along the entire length of the microcomposite. Such fibre-to-fibre damage correlation occurs very quickly, even at large interfibre distances, and the load sharing mechanism may therefore be viewed, in this kevlar 149 based composite system, as equal load sharing (ELS) among the fibres, a conclusion similar to the one obtained earlier from the results at low applied strains. Thus, the overloading of an intact fibre due to load released by a neighbouring broken fibre is short-lived, or transient, since the intact fibre ruptures very quickly. We saw earlier that such overloading seems to be relatively small, so the key question becomes: why are neighbouring intact fibres so sensitive (or prone to fracture) under relatively small stress concentration factors, and even at large (12D) distances? The answer is perhaps the following. Using scanning electron microscopy (SEM), the surface of kevlar 149 single fibres was found [32] to contain a large density of defects, arranged in a helicoidal fashion along the fibre length. These defects may be observed by optical microscopy at high magnification, see for example some of the fibres that appear in the photograph on Fig. 1c. They play a role of high "stress concentrators" and are the cause of the sensitivity of these fibres to any local load increase, even when large interfibre distances exist. In such case, it appears therefore that fibre–fibre interactions may exist at large interfibre distance, even though such interaction is barely detectable in terms of the stress concentration factors.

Finally, the so-called 'critical cluster size', beyond which final fracture of the composite occurs in a catastrophic manner, could not be observed here, and it can only be stated that this cluster size is definitely larger than 5 in kevlar 149–urethane–acrylate composites, for all interfibre distances studied.

4. Conclusions

We have used laser micro-Raman spectroscopy to study the extent of stress transfer and redistribution caused by fibre fracture in two-dimensional kevlar 149 based microcomposites. The strain along the fibres was mapped at different strain levels, and specimens with different inter-fibre distances (from 2 to 12 fibre diameters) were used to study the fibre content effect. The experimental stress concentration factors were compared with values predicted from various theoretical models. It was found that the stress concentration factors were lower than those observed previously and generally agreed with those literature models that include interfibre distance and matrix effects. The overall failure pattern was found not to be a direct function of the stress concentration factors in this system, as fracture propagates from fibre to fibre even at large interfibre distances, and is apparently accompanied by relatively low values of the stress concentration factors. The 'critical cluster size', beyond which final fracture of the composite occurs in a catastrophic manner, was found to be larger than 5 in the present system, for all interfibre distances studied.

Acknowledgements

This work was supported in part by the Stein Foundation at Drexel University.

References

1. H. D. WAGNER and A. EITAN, *Appl. Phys. Lett.* **58** (1991) 1033.
2. *Idem, Composites Science and Technology*, **46** (1993) 353.
3. H. E. DANIELS, *Proc. Roy. Soc. London* **A183** (1945) 404.
4. J. M. HEDGEPETH, NASA TN D-882 (1961).
5. J. M. HEDGEPETH and P. VAN DYKE, *J. Compos. Mater.* **1** (1967) 294.
6. W. B. FICHTER, NASA TN D-5453 (1969).
7. D. G. HARLOW and S. L. PHOENIX, *J. Compos. Mater.* **12** (1978) 195.
8. *Idem, ibid.* **12** (1978) 314.
9. R. E. PITT and S. L. PHOENIX, *Int. J. Fracture* **20** (1982) 291.
10. *Idem, ibid.* **22** (1983) 243.
11. R. L. SMITH, S. L. PHOENIX, M. GREENFIELD, R. B. HENSTENBURG and R. E. PITT, *Proc. Roy. Soc. London* **A388** (1983) 353.
12. H. FUKUDA and K. KAWATA, *Fukugo Zairyo Kenkyu (Comp. Mater. Struct.)* **3** (1974) 21.
13. *Idem. Fibre Sci. Technol.* **9** (1976) 189.
14. *Idem. ibid* **10** (1977) 53
15. J. N. ROSSETTOS and M. SHISHESAZ, *J. Appl. Mech.* **54** (1987) 723.
16. M. G. BADER, R. L. SMITH, M. J. PITKETHLY, Proc. Sixth Intern. Confer. on Composite Materials (ICCM-6) & Second Europ. Confer. on Composite Materials (ECCM-2) (F. L. Matthews, N. C. R. Buskell, J. M. Hodgkinson, J. Morton, Eds), 20–24 July, 1987, London (Elsevier Applied Science, London, 1987), Vol. 5 (1987) 481.
17. D. A. CLARKE and M. G. BADER, *ibid.* Vol. 5, (1987) 382.
18. *Idem*, in Proc. 7th Intern. Confer. on Composite Materials (ICCM-7) 25–28 August, 1989, Beijing (Eds: Wu Yunshu, Gu Zhenlong, and Wu Renjie, Intern. Acad. Publish., Beijing, Pergamon Press, Oxford, UK, 1989), Vol. 2. p. 79.
19. L. C. WOLSTENHOLME and M. G. BADER, *ibid*, Vol. 2, p. 84.
20. L. C. WOLSTENHOLME and R. L. SMITH, *J. Mater. Sci.* **24** (1989) 1559.

21. M. R. NEDELE and M. R. WISNOM, *Composites Science and Technology* **51** (1994) 517.
22. N. MELANITIS, C. GALIOTIS, P. TETLOW and C. DAVIES, *J. Mater. Sci.* **28** (1993) 1648.
23. R. J. YOUNG, in Polymer Surfaces and Interfaces II (W. J. Feast, H. S. Munro, R. W. Richards, Eds), John Wiley & Sons (1993), pp. 131–159.
24. L. SCHADLER, C. LAIRD, N. MELANITIS, C. GALIOTIS and J. FIGUEROA, *J. Mater. Sci.* **27** (1992) 1663.
25. H. D. WAGNER and L. W. STEENBAKKERS, *ibid* **24** (1989) 3956.
26. H. D. WAGNER, M. RUBINS and G. MAROM, *Polym. Compos.* **12** (1991) 233.
27. R. GULINO, P. SCHWARTZ and S. L. PHOENIX, *J. Mater. Sci.* **26** (1991) 6655.
28. Z.-F. LI, D. T. GRUBB and S. L. PHOENIX, *J. Mater. Sci. Lett.* **13** (1994) 1720.
29. K. M. ATALLAH and C. GALIOTIS, *Composites* **24** (1993) 635.
30. B. YAVIN, H. E. GALLIS, J. SCHERF, A. EITAN and H. D. WAGNER, *Polymer Composites* **12** (1991) 436.
31. H. D. WAGNER, in "Application of Fracture Mechanics to Composite Materials" (K. Friedrich, Editor, R. B. Pipes, Composite Materials Series Editor), Composite Materials Series 6, Elsevier Science Publishers B. V., Amsterdam, 1989, pp. 39–77.
32. L. W. STEENBAKKERS and H. D. WAGNER, *J. Mater. Sci. Lett.* **7** (1988) 1209.

Received 10 April 1995
and accepted 8 September 1995